Nonadiabatic spin-transfer torque of magnetic vortex structures in a permalloy square

Stefan Rößler,[1] Sebastian Hankemeier,[1,*] Benjamin Krüger,[2] Felix Balhorn,[1] Robert Frömter,[1] and Hans Peter Oepen[1]

[1]*Universität Hamburg, Institut für Angewandte Physik, Jungiusstr. 11, 20355 Hamburg, Germany*
[2]*Institut für Physik, Johannes Gutenberg Universität Mainz, Staudinger Weg 7, 55128 Mainz, Germany*

The stationary displacement of a magnetic vortex core in a permalloy square caused by an ultrahigh direct current has been measured utilizing scanning electron microscopy with polarization analysis. Data have been analyzed for three different generic states of the Landau structure and up to a current density of $3 \times 10^{11} \mathrm{A/m^2}$. This procedure allows for separating the effects caused by the Oersted field, the nonadiabatic, and the adiabatic spin-transfer torque. In addition, the spin polarization of the driving current $P = (65 \pm 4)\%$ is independently determined from the spin drift velocity of $v_j = (4.79 \pm 0.26)\,\mathrm{m/s}$ at $j = 1 \times 10^{11}\,\mathrm{A/m}$. Ferromagnetic resonance measurements have been conducted to complete the set of parameters for our film system $(\alpha, g, M_\mathrm{S})$. The full set of parameters allows for a direct comparison of the nonadiabatic spin-transfer torque with previously published results. In contrast to published values in the range of the damping parameter, a strongly increased value of $\beta = 0.119 \pm 0.022$ as a parameter of nonadiabaticity is found, which supports recent theoretical predictions of an additional nonlocal spin-transfer torque contribution effective at the vortex structure.

I. INTRODUCTION

Triggered by the advent of a new concept of data storage via magnetic domain walls [1], the manipulation of domain walls with electric current has become an issue of great interest [2]. The interaction of a current with a magnetic microstructure is described in the framework of the Landau-Lifshitz-Gilbert (LLG) equation [3,4]. The latter equation is commonly extended to include the effect of an electrical current via two additional terms describing the adiabatic and nonadiabatic contributions [5–8]. The nonadiabatic contribution is phenomenologically covered via the parameter of nonadiabaticity β. Both, the velocity of a domain wall [9] and the critical current for domain wall movement [9] depend on β. Thus, the exact determination of β is crucial for the optimization of material systems for the above-mentioned new memory devices.

The parameter of nonadiabaticity, however, is an issue of long-standing debate. The published values for permalloy vary over several orders of magnitude [2,10–12]. Most of the results have been obtained with experiments that investigate the movement of so-called "domain walls" in magnetic nanowires built from soft-magnetic materials. In contrast to early one-dimensional theoretical models, these domain walls in general have a more complex internal structure, called vortex or transverse walls. The results appear to depend strongly on the geometry, the microstructure, and pinning due to imperfections of the wire, which strongly contributes to the large span of reported β values. To overcome the latter problems, a robust measurement scheme was proposed by Krüger *et al.* in 2010 [13] based on the measurement of the current-induced displacement of a magnetic vortex core in a square magnetic element.

First measurements based on this approach have been performed utilizing permalloy discs [14]. The disc geometry offers the highest probability to obtain a magnetic vortex as equilibrium microstructure. Its major drawback, however, is the inhomogeneous current density that has to be expected due to the geometry of the structure. The varying current distribution puts limits on the exact analysis based on a macroscopic, Thiele-like approach [13]. Consequently, a relatively high uncertainty of the measured value ($\beta = 0.15 \pm 0.07$) [14] is obtained. Pollard *et al.* [15] measured the orbit of a harmonically exited vortex and claim to determine β with higher precision ($\beta = 0.15 \pm 0.02$). The error margins given in this publication, however, are not well founded, as the authors did not determine all necessary material parameters. The largest uncertainty stems from the spin polarization of the current, for which published values vary by a factor of two [16]. This course of action has been criticized in a recent paper, and the necessity to determine the material parameters in one and the same experiment for the same sample has been put forward [17].

From the theoretical point of view, the large spread of experimental values for the nonadiabaticity caused a re-examination of the nonadiabatic spin-transfer torque. In general, the microstructure in small wires, called the "domain wall," has a large extent, and the truly nonadiabatic effect should not appear [18]. With dynamical damping being the only contribution, β will be of the same order as the damping parameter [18–20]. In fact, in recent papers studying spin waves, nonadiabaticity values in the range of the damping constant have been found [21,22]. In the latter publications the authors make a complete analysis in the sense of Lepadatu [17] (i.e., they determine all necessary parameters to characterize their films in full). That finding lets the question arise whether the former "incomplete" investigations on vortices and vortex walls that came up with a much larger β value can be confirmed and how they can be understood.

In this paper, we present the results of an investigation in which all three parameters α, β, and P are determined independently. Our method utilizing scanning electron microscopy with polarization analysis (SEMPA) follows the proposed robust scheme [13]. We determine β without any

———
*Present address: Tesat-Spacecom GmbH & Co. KG, Gerberstr. 49, 71522 Backnang, Germany.

assumptions on spin polarization or damping. Furthermore, we independently determine the spin polarization of the current within the same set of experiments.

II. THEORETICAL APPROACH

For a current flowing in the x direction (electrons moving in a negative x direction) the LLG equation reads [3–8]

$$\dot{\boldsymbol{m}} = -\gamma \boldsymbol{m} \times \boldsymbol{H}_{\text{eff}} + \alpha \boldsymbol{m} \times \dot{\boldsymbol{m}} + v_j \frac{\partial \boldsymbol{m}}{\partial x} - \beta v_j \boldsymbol{m} \times \frac{\partial \boldsymbol{m}}{\partial x}, \quad (1)$$

with Gilbert damping α and the effective field $\boldsymbol{H}_{\text{eff}}$ consisting of external, demagnetization, anisotropy, and exchange fields. Also included are the parameter of nonadiabaticity β and the spin drift velocity v_j,

$$v_j = \frac{g\mu_{\text{B}}P}{2eM_{\text{S}}} j, \quad (2)$$

which parameterizes the strength of the interaction and includes the spin polarization of the conduction electrons P.

Many problems in experiments that try to determine the β parameter arise from the separation of the different contributions that originate from the adiabatic and nonadiabatic spin-transfer torques, the Oersted field, and an inhomogeneous current flow. In time-resolved experiments utilizing short current pulses, the impact of rise time and duration of the pulses on the temporal evolution of resistance and lateral temperature profile (and implicitly on pinning processes) are to a large extent not specified [13,23]. To avoid most of these uncertainties, a stationary experiment has been proposed in which the equilibrium displacement of a vortex core in a square structure by a direct current is determined [13]. The displacement depends on the magnetic configuration of the vortex structure (i.e., the sense of rotation and polarity of the vortex core). The latter feature bears the power to separate the contributions caused by the Oersted field and the adiabatic as well as the nonadiabatic spin-transfer torque. As only small displacements are considered in the experiments, edge roughness and imperfections can be neglected [13]. Also, one should note that in a stationary experiment, local pinning of the vortex core will only increase the statistical error of a data set. This is different for a dynamic experiment, as frequent pinning and depinning of the vortex can lead to additional damping due to the generation of spin waves, which results in a systematic error.

A sketch of the sample geometry, as well as the definition of the coordinate system, is given in Fig. 1. The magnetic vortex is described by its core polarity p, being positive for core magnetization pointing in $+z$ direction, and its rotational sense c, being positive for counterclockwise rotation when looking at the sample from above ($z > 0$).

The equilibrium position $\boldsymbol{R}$ of a magnetic vortex core under current flow can be written as a two-dimensional vector [13]

$$\boldsymbol{R}_c^p(j) = -\frac{|G_0|}{m\omega_r^2} \begin{pmatrix} \tilde{H}c + \left|\frac{D_0}{G_0}\right| \xi v_j \\ v_j p \end{pmatrix}, \quad (3)$$

with G_0, the z component of the gyrovector, and $m\omega_r^2$ parameterizing the confining potential. The first contribution to the displacement in the x direction is due to the Oersted
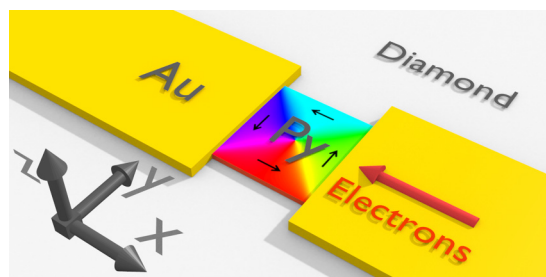

FIG. 1. (Color online)   Schematic of the sample layout. A permalloy square of edge length 5 μm is prepared on a single-crystalline diamond and contacted by gold leads. The diamond guarantees best thermal conductivity. The vortex core in the center of the magnetic structure is displaced by a direct current. The displacement is mapped via SEMPA.

field $\tilde{H}$. The direction of this displacement depends on the sense of rotation c of the vortex core. A second contribution comes from the nonadiabatic spin-transfer torque consisting of the diagonal element of the dissipation tensor D_0 and ξ, with $\beta = \frac{\xi}{1+\xi^2}$. Displacement in the y direction is solely caused by the adiabatic spin-transfer torque, which depends directly on the polarity of the vortex core p and the spin drift velocity v_j. Comparing the displacement of two vortices with different senses of rotation, the different contributions can be separated. The parameter of interest can be extracted according to the formula [13,14]

$$\xi = \frac{1}{2}\frac{G_0}{D_0}\left(p\frac{dx}{dy}(c,p) + p\frac{dx}{dy}(-c,p)\right). \quad (4)$$

The equation for the displacement of the vortex core includes some material properties that have to be determined independently for the sample that is studied. In particular, the factors $\frac{|G_0|}{m\omega_r^2}$ and $\frac{D_0}{G_0}$ depend on the saturation magnetization (and therefore on temperature) and on sample geometry (film thickness), which means that to get rid of all the uncertainties that can and will influence the data found in literature, it is strongly advised to determine all the parameters of the experiment and the sample.

III. EXPERIMENTAL DETAILS

To determine the vortex core position at ultrahigh current densities with high precision we used SEMPA [24–27]. Due to a low efficiency of the polarization analysis, typical times for taking an image are in the range of a few minutes, which means that the ultrahigh current densities have to be applied over extended periods. To meet this prerequisite, the permalloy square is fabricated on a single-crystalline diamond substrate [28]. Due to the high thermal conductivity of diamond [29], an efficient connection to a heat sink is ensured, which prevents excessive heating of the structure during current flow.

The sample consists of a magnetic square that is connected to bond pads by gold leads. All films are prepared by thermal evaporation at room temperature. In the first preparation step, two Pt/Cr bond pads with a separation of 20 μm are deposited. Next, the permalloy square of size 5000 × 5000 × 12 nm^3 is deposited between them utilizing a stencil mask. A second
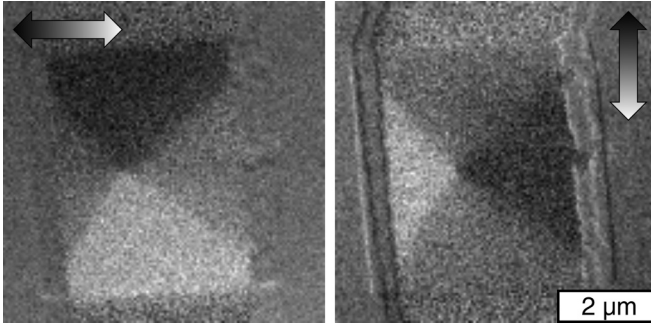
FIG. 2.　　SEMPA image (128×128 pixels, dwell time 15 ms) of the Py square at zero applied current. Both images have been obtained simultaneously and show the x and y components of the in-plane magnetization, respectively (see arrows). The as-grown structure exhibits a Landau state with sense of rotation $c = +1$.
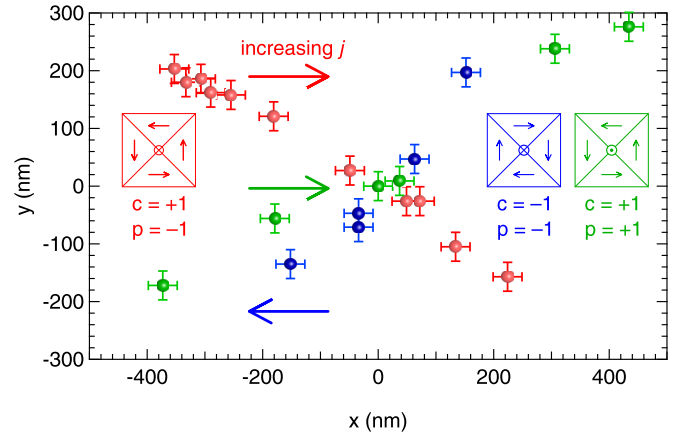

FIG. 3. (Color online)　　Current-induced displacements of the vortex core for three configurations of the Landau state. The current density has been varied in the range of $j = \pm 3 \times 10^{11}$ A/m^2. The vortex core moves along a line in this representation. Displacements caused by a constant background field (~ 0.5 mT) have been eliminated (see text).

mask is then used to evaporate two gold leads (thickness 15 nm) that close the gap between the square and bond pads for an electrical connection. Finally, the diamond is mounted on a polished copper plate.

　　Figure 2 shows a SEMPA image of the magnetic structure, a Landau state, in the as-prepared state with a sense of rotation of $c = +1$. During the course of the investigation the sense of rotation was changed by applying an *in situ* demagnetizing cycle. The polarity can be set by applying a field with a small z component during the latter procedure. Using this approach, three different Landau states have been generated.

　　Due to the high surface sensitivity of the spin-polarized secondary electron emission, the measuring time is limited even in ultrahigh vacuum (base pressure 4×10^{-11} mbar). In the case of Py, the latter base pressure allows for a typical measurement time of hours before the signal gets too faint due to contamination by residual gases [30]. The sample has to be cleaned after that time span. During the course of the investigation presented here, cleaning via ion milling (1 keV, Ar) was performed four times. After each of the necessary cleaning steps, the thickness of the Py square is slightly reduced. The film thickness before $t_i = (11.8 \pm 0.2)$ nm and after $t_f = (6.4 \pm 0.2)$ nm was determined via atomic force microscopy (AFM). The value at the end of the investigation has been corrected by accounting for some removal of diamond utilizing a tabulated sputtering yield of diamond [31]. Assuming a linear decrease of film thickness with ion dose, Py thicknesses for the individual measurements were calculated (i.e., $t_1 = 9.6$ nm, $t_2 = 8.5$ nm, and $t_3 = 7.3$ nm). These thicknesses fit quite well with the evolution of the electrical resistances after each milling. Direct current densities within the range $\pm 3 \times 10^{11}$ A/m^2 have been applied during the investigation.

　　The temperature of the sample is determined via its resistance. The resistance calibration has been performed in thermal equilibrium while slowly cooling down to 80 K with LN$_2$. Utilizing the latter calibration curve, the temperature and its variation has been determined to be $T = (341 \pm 9)$ K during measurement (without applied cooling). As each measurement cycle is started with the highest current density $j_{\max}$, the temperature first increases to $T \approx 350$ K. On changing the current density in equal steps to $-j_{\max}$ the temperature profile is that

of a parabola with a minimum of T ≈ 332 K at zero current. The parabola is shifted with respect to room temperature due to heating of the sample holder. It was recently shown that a temperature variation of that magnitude has no effect on the nonadiabatic spin-transfer torque in permalloy [32].

IV. EXPERIMENTAL RESULTS

　　In Fig. 3 the y versus x displacements are plotted for the three different Landau configurations for varying current densities. Obviously, the position of the vortex core follows a linear trajectory in this presentation. From Eq. (3) it immediately follows that the Oersted contribution must depend linearly on current density. The Oersted field is caused by a vertically inhomogeneous current flow in the sample [33] and the geometry of the contact leads [34]. Furthermore, the sign of the slope is given by the product of sense of rotation and core polarization cp, which indicates that the Oersted field contribution in the displacement along the x direction is dominant. In the as-grown state ($c = +1$, $p = -1$, red crosses) we find that the vortex core is displaced in the negative x direction for increasing currents (positive current flowing from left to right). This indicates that the Oersted field is pointing in the positive y direction, as it is favoring the right domain in Fig. 1. The nonadiabatic spin-transfer torque drives the vortex core in the negative x direction for increasing current densities (i.e., the direction of electron flow). Displacement in the y direction is solely caused by the adiabatic spin-transfer torque. Since the core is displaced toward lower y values for increasing current densities, the polarity of the vortex core is $p = -1$ according to Eq. (3). Two more magnetic states (i.e., $c = -1$, $p = -1$ and $c = +1$, $p = +1$; represented by blue and green crosses in Fig. 3) reveal a similar behavior in accordance with Eq. (3).

　　The equilibrium position of the vortex core (Fig. 3) was corrected for displacements due to a small residual field (~ 0.5 mT), which is generated by the objective lens of the SEM column and points in the y direction. As the

TABLE I. Vortex core displacement per unit current density $j_0 = 10^{11}$ A/m^2 obtained from Fig. 3. For the sake of better comparison, the values are divided by the thickness-dependent confining potential $a = G_0/m\omega_r^2$. The such-corrected displacement in the y direction is the spin drift velocity v_j, which is constant within the error margin. The amplitude of the displacement in the x direction is larger when the nonadiabatic spin-transfer torque and the Oersted field act in the same direction ($c = +1$) compared with the case of opposite action ($c = -1$). The fact that the amplitude in the x direction for Nos. 1 and 3 (identical $c = +1$) increases with decreasing thickness reveals that the Oersted field gets stronger with reduced thickness [54].

No.	c	p	t (nm)	$1/a$ (MHz)	$x(j_0)/a$ (m/s)	$y(j_0)/a$ (m/s)
1	$+1$	-1	9.6 ± 0.2	99 ± 5	-7.8 ± 0.5	4.8 ± 0.4
2	-1	-1	8.5 ± 0.2	88 ± 4	4.0 ± 0.5	4.6 ± 0.5
3	$+1$	$+1$	7.3 ± 0.2	76 ± 4	-9.8 ± 0.7	-5.1 ± 0.4

position of the vortex depends on the sense of rotation and film thickness, the equilibrium was determined for each measurement independently. For that purpose, equilibrium positions were calculated via $\boldsymbol{R}_{\mathrm{eq}} = \frac{1}{2}(\boldsymbol{R}(+j) + \boldsymbol{R}(-j))$. The average over all values, including the value when no current is applied ($\boldsymbol{R}(j = 0)$), is taken as the equilibrium position. Since only the slope of the trajectories enters in the determination of the experimental parameters, this correction is not critical.

A. Determination of v_j and P

From linear fits to the data presented in Fig. 3, displacements for the given current are calculated and given in Table I. All values are divided by the prefactor $a = \frac{|G_0|}{m\omega_r^2}$ to eliminate the thickness dependence of the confining potential (see the Appendix). The error margins are determined by considering the uncertainties in vortex position, film thickness, lateral dimension, and stability of the current.

The spin drift velocity v_j (i.e., the displacement in the y direction divided by $a = \frac{|G_0|}{m\omega_r^2}$) is constant within the error margin (last column in Table I). The mean value is $v_j = (4.79 \pm 0.26)$ m/s for $j = 1 \times 10^{11}$ A/m at $T = (341 \pm 9)$ K.

The method applied here gives direct access to the spin drift velocity without any further assumptions. Spin drift velocities can also be directly obtained from measurements of the Doppler shift of spin waves. Published data for identical current densities are $v_j = 4.1 \pm 0.1$ m/s (at 340 K) [16] and $v_j = 5.0$ m/s [21,35]. Within the temperature uncertainty we can conclude excellent agreement. As the values of v_j (last column in Table I) do not reveal any systematic change with thickness, it can be concluded that the magnetic properties of the films are not altered by the ion milling.

The spin drift velocity v_j gives access to the spin polarization of the conduction electrons [9]. For that purpose, the saturation magnetization and the gyromagnetic ratio of the system under investigation have to be known. To eliminate any uncertainty, we have performed ferromagnetic resonance measurements utilizing a reference film that has been grown simultaneously. Fitting the resonance line as presented in Ref. [36], we obtain for the least square fit $M_S = (824 \pm 5)$ kA/m, $\alpha = (0.0085 \pm 0.0006)$, and g $= 2.071 \pm 0.005$

at room temperature. Extrapolating to the M_S value at the somewhat elevated temperature [37], we can determine the spin polarization of $P = (65 \pm 4)\%$, which is in fairly good agreement with the values from Doppler measurements [16].

B. Determination of ξ and β

The quantity that depends on the ξ parameter is the displacement in the x direction. In general, the Oersted field contribution is eliminated by summing up the displacements along the x direction for two vortices with opposite sense of rotation, as shown in Eq. (4). It is striking that the x displacement values are different for identical c, while the y displacements are the same within the error margins. The variation of the x values originates predominantly from the contribution due to Oersted fields, while a weak thickness dependence can be expected for the nonadiabaticity term [Eq. (3)] via the prefactor $\frac{|D_0|}{|G_0|}$ (see Appendix). To eliminate the Oersted field contribution, it is necessary to determine the x displacement for $c = \pm 1$ at the same thickness. For that purpose, an estimation for the x displacement at the intermediate thickness ($t = 8.5$ nm) for positive sense of rotation ($c = +1$, $p = -1$) is made based on the values for the positive sense of rotation at the lower and higher thicknesses, i.e., $dx/dy(c = +1, p = -1, t = 9.6$ nm$) = -1.63 \pm 0.14$ and $-dx/dy(c = +1, p = +1, t = 7.3$ nm$) = -1.93 \pm 0.16$ (Table I). Assuming a monotonous change with thickness, the calculation gives a value for the slope of $dx/dy(c = +1, p = -1, t = 8.5$ nm$) = -1.78 \pm 0.10$. Utilizing Eq. (4), the nonadiabaticity ξ is calculated from the extrapolated and measured values, i.e., $dx/dy(c = -1, p = -1, t = 8.5$ nm$) = 0.87 \pm 0.14$ (second row Table I), considering $\frac{|D_0|}{|G_0|} = 3.75$ for a thickness of 8.5 nm:

$$\xi = 0.121 \pm 0.023,$$
$$\beta = 0.119 \pm 0.022.$$

A similar consideration gives the value for $\tilde{H}/v_j = 1.33 \pm 0.16$ for that thickness, which corresponds to an effective field of 44 μT for $j = 1 \times 10^{11}$ A/m. Finally, as the Oersted contribution is predominant, the values given in Table I reveal the thickness dependence of the Oersted field. Its contribution to the vortex displacement increases with decreasing thickness [54].

V. DISCUSSION

In our investigation, the spin drift velocity, the spin polarization, and the β parameter have been determined from a single stationary-state experiment. The latter quantities are determined without any assumptions on and independent from transient temperature profiles and/or damping processes. In combination with the independently measured saturation magnetization and damping parameter, we have all relevant material parameters of the system at hand, which allows for a strict comparison to previously published data. First, it has to be emphasized that the β parameter found here is almost the same as in the two previous experiments utilizing magnetic vortices in microstructures [14,15]. As the error bars in the

previous experiments were large or nonproven assumptions were made (e.g., about spin polarization), our findings have their relevance and self-reliance in the accurateness of the experiments. Second, our data supports the assumption of $P = 60\%$ in the paper by Pollard *et al.* [15], albeit the reported damping parameters disagree considerably, indicating that the β values determined here and in Refs. [14,15] are independent of damping. However, this conclusion can only be drawn assuming that the damping parameter is independent of magnetic structure, which is currently under debate [38].

Third, Sekiguchi *et al.* [21] did a complete analysis of their system, which allows for comparison on firm grounds. The authors report almost identical numbers for the damping parameter, spin drift velocity and spin polarization, while the nonadiabaticity parameter is much smaller ($\beta = 0.022$) than the value found here ($\beta = 0.119 \pm 0.022$). Fourth, all the other investigations on the nonadiabatic spin-transfer torque come about with more or less strong deviations from our results. This obviously stems from the different structures that are used, which will be more or less affected by pinning, while in general not all relevant parameters have been determined simultaneously [39–45].

Theory predicts two different contributions to β [19]: the true nonadiabatic contribution due to spin scattering [6] and a magnetic-damping–related transfer of momentum [7,18]. The former depends on the gradient of the magnetization along the current direction [46,47] and is essentially of nonlocal nature, while the latter scales with damping [18,48]. In other words, the first effect needs strong magnetization gradients while the latter does not. Sekiguchi *et al.* [21] analyzed spin waves with a characteristic length scale of magnetization variation of 10 μm. On such large scales only the damping-related nonadiabatic contribution will cause the spin-transfer torque. Consistently the authors find a ratio β/α in the range of unity ($\beta/\alpha = 2$). In accordance with this interpretation and stressing the fact that the material parameters are almost identical in both investigations, we may conclude that the present investigation proves and quantifies experimentally the existence of two contributions to β. The latter conclusion is strictly valid, as the only difference between the two samples investigated is the gradient of the magnetization structure at the vortex core.

The potentially strong influence of a nonlocal, nonadiabatic correction in vortex structures has been proposed by theory [46,49]. A seven times stronger effective β has been reported in an experiment comparing vortex with transverse walls [50]. Recently, an iterative micromagnetic simulation of nonlocal spin-transfer torque in the framework of Zhang and Li [6] has been published by Claudio-González *et al.* [51]. The authors include spin diffusion and accumulation and could demonstrate that, in case of a transverse wall, no significant deviations from a homogeneous β could be found while the strong magnetization gradient originating at the core of a vortex wall increases the locally acting β by almost a factor of three. In such a nonlocal picture the β value determined by our analysis has to be interpreted as a properly weighted average over the spatial distribution of the locally varied values in a way similar to the effective β_{diff} calculated in Ref. [51]. Our experiment offers a reliable set of data to test the adequacy of such a new simulation scheme, as

it is not systematically disturbed by extrinsic effects like pinning. The stationary-state solution will allow simulation with less calculative effort compared with a gyrating system. Alternatively, a nonlocal reformulation of the Thiele equation ansatz, which leads to Eq. (3), can be attempted. Once a refined model becomes available, our data can be used to extract the diffusion constant of electrons in permalloy and to test for consistency.

VI. SUMMARY AND CONCLUSION

In a stationary-state experiment the β parameter of a Landau pattern and the spin drift velocity are determined independently. A value of $\beta = 0.119 \pm 0.022$ is found for a magnetic vortex core displaced by a direct current in the theoretical framework of local spin-transfer torques. A spin polarization of $P = (65 \pm 4)\%$ is deduced from a spin drift velocity of $v_j = (4.79 \pm 0.26)$ m/s at a current density of $j = 1 \times 10^{11}$A/m^2. Our experiment proves and quantifies the strong increase of the nonadiabatic spin-transfer torque that is effective at magnetic vortices—a finding that is presently attributed to the nonlocal contribution from spin-flip scattered conduction electrons. Our complete set of data can be used to validate recent simulations in the quest for a unified description of spin-transfer torque with the predictive power required in technological application engineering.

APPENDIX: MICROMAGNETIC SIMULATIONS

The dependence of the prefactors $\frac{|G_0|}{m\omega_r^2}$ and $\frac{D_0}{G_0}$ on M_{S} has been extracted from simulations in the range of 800 kA/m $\leq M_{\text{S}} \leq$ 890 kA/m for the three measured thicknesses in steps of $\Delta M_{\text{S}} = 30$ kA/m. Simulations were performed using MicroMagnum [52] with a cell size of $2 \times 2 \times t$ nm^3 and $A = 13 \times 10^{-12}$J/m for permalloy. Square structures with an edge length in the range of 500 nm $\leq l \leq$ 1700 nm were used in the simulation. The data for the confining potential was calculated from the vortex displacement in the y direction. It was best fit by

$$\frac{m\omega_r^2}{2} = 0.9\frac{\mu_0 M_{\text{S}}^2 t^2}{l} + 65\frac{\text{pJ}}{\text{m}} \times \frac{t + 8.5 \text{ nm}}{l^2}. \quad (\text{A1})$$

The values of G_0 can be found in Ref. [53]. Results for the inverse of the confining potential of our sample $m\omega_r^2/G_0$ are found in Table I. With $\alpha^2 \ll 1$, they correspond to the resonance frequency of the vortex core $2\pi f_{\text{res}}$ [53].

The data for $\frac{D_0}{G_0}$ was extracted from the ratio of x and y displacements and is best fit by

$$\frac{D_0}{G_0} = \frac{1}{2}\ln\left(\frac{1.85}{\text{nAm}}l\left(M_{\text{S}} + 220\frac{\text{kA}}{\text{m}}\right)(97 \text{ nm} - t)\right)$$
$$+ \frac{27.7}{\mu\text{Am}}(t + 2 \text{ nm})\left(M_{\text{S}} - 550\frac{\text{kA}}{\text{m}}\right)l. \quad (\text{A2})$$

[1] S. S. P. Parkin, M. Hayashi, and L. Thomas, Science **320**, 190 (2008).

[2] G. Beach, M. Tsoi, and J. Erskine, J. Magn. Magn. Mater. **320**, 1272 (2008).

[3] L. Landau and E. Lifshitz, Phys. Z. Sowjetunion **8**, 153 (1935).

[4] T. Gilbert, Phys. Rev. **100**, 1243 (1955); IEEE Trans. Magn. **40**, 3443 (2004).

[5] Y. B. Bazaliy, B. A. Jones, and S. C. Zhang, Phys. Rev. B **57**, R3213 (1998).

[6] S. Zhang and Z. Li, Phys. Rev. Lett. **93**, 127204 (2004).

[7] G. Tatara and H. Kohno, Phys. Rev. Lett. **92**, 086601 (2004).

[8] A. Thiaville, Y. Nakatani, J. Miltat, and N. Vernier, J. Appl. Phys. **95**, 7049 (2004).

[9] A. Thiaville, Y. Nakatani, J. Miltat, and Y. Suzuki, Europhys. Lett. **69**, 990 (2005).

[10] G. S. D. Beach, C. Knutson, C. Nistor, M. Tsoi, and J. L. Erskine, Phys. Rev. Lett. **97**, 057203 (2006).

[11] M. Hayashi, L. Thomas, C. Rettner, R. Moriya, X. Jiang, and S. S. P. Parkin, Phys. Rev. Lett. **97**, 207205 (2006).

[12] M. Hayashi, L. Thomas, C. Rettner, R. Moriya, and S. S. P. Parkin, Nat. Phys. **3**, 21 (2007).

[13] B. Krüger, M. Najafi, S. Bohlens, R. Frömter, D. P. F. Möller, and D. Pfannkuche, Phys. Rev. Lett. **104**, 077201 (2010).

[14] L. Heyne, J. Rhensius, D. Ilgaz, A. Bisig, U. Rüdiger, M. Kläui, L. Joly, F. Nolting, L. J. Heyderman, J. U. Thiele, and F. Kronast, Phys. Rev. Lett. **105**, 187203 (2010).

[15] S. Pollard, L. Huang, K. Buchanan, D. Arena, and Y. Zhu, Nat. Commun. **3**, 1028 (2012).

[16] M. Zhu, C. L. Dennis, and R. D. McMichael, Phys. Rev. B **81**, 140407 (2010).

[17] S. Lepadatu, M. C. Hickey, A. Potenza, H. Marchetto, T. R. Charlton, S. Langridge, S. S. Dhesi, and C. H. Marrows, Phys. Rev. B **79**, 094402 (2009).

[18] I. Garate, K. Gilmore, M. D. Stiles, and A. H. MacDonald, Phys. Rev. B **79**, 104416 (2009).

[19] G. Tatara and P. Entel, Phys. Rev. B **78**, 064429 (2008).

[20] K. Gilmore, I. Garate, A. H. MacDonald, and M. D. Stiles, Phys. Rev. B **84**, 224412 (2011).

[21] K. Sekiguchi, K. Yamada, S.-M. Seo, K.-J. Lee, D. Chiba, K. Kobayashi, and T. Ono, Phys. Rev. Lett. **108**, 017203 (2012).

[22] J.-Y. Chauleau, H. G. Bauer, H. S. Körner, J. Stigloher, M. Härtinger, G. Woltersdorf, and C. H. Back, Phys. Rev. B **89**, 020403(R) (2014).

[23] L. Bocklage, B. Krüger, T. Matsuyama, M. Bolte, U. Merkt, D. Pfannkuche, and G. Meier, Phys. Rev. Lett. **103**, 197204 (2009).

[24] R. Frömter, S. Hankemeier, H. P. Oepen, and J. Kirschner, Rev. Sci. Instrum. **82**, 033704 (2011).

[25] K. Koike and K. Hayakawa, Jpn. J. Appl. Phys. **23**, L187 (1984).

[26] J. Unguris, D. T. Pierce, and R. J. Celotta, Rev. Sci. Inst. **57**, 1314 (1986).

[27] H. P. Oepen and J. Kirschner, Scanning Microsc. **5**, 1 (1991); J. Phys. (Paris) **49**, 1853 (1988).

[28] S. Hankemeier, K. Sachse, Y. Stark, R. Frömter, and H. P. Oepen, Appl. Phys. Lett. **92**, 242503 (2008).

[29] S. Barman and G. P. Srivastava, J. Appl. Phys. **101**, 123507 (2007).

[30] F. Lofink, S. Hankemeier, R. Frömter, J. Kirschner, and H. P. Oepen, Rev. Sci. Instrum. **83**, 023708 (2012).

[31] T. J. Whetten, A. A. Aemstead, T. A. Grzybowski, and A. L. Ruoff, Vac. Sci. Technol. **2**, 477 (1983).

[32] B. Beyersdorff, S. Hankemeier, S. Rößler, Y. Stark, G. Hoffmann, R. Frömter, H. P. Oepen, and B. Krüger, Phys. Rev. B **86**, 184427 (2012).

[33] H. Fangohr, D. S. Chernyshenko, M. Franchin, T. Fischbacher, and G. Meier, Phys. Rev. B **84**, 054437 (2011).

[34] K.-W. Moon, J.-C. Lee, K. Rhie, K.-H. Shin, and S.-B. Choe, IEEE Trans. Magn. **47**, 2508 (2011).

[35] V. Vlaminck and M. Bailleul, Science **322**, 410 (2008).

[36] S. S. Kalarickal, P. Krivosik, M. Wu, C. E. Patton, M. L. Schneider, P. Kabos, T. J. Silva, and J. P. Nibarger, J. Appl. Phys. **99**, 093909 (2006).

[37] J. Crangle and G. C. Hallam, Proc. R. Soc. Lond A, **272**, 119 (1963).

[38] J. Foros, A. Brataas, Y. Tserkovnyak, and G. E. W. Bauer, Phys. Rev. B **78**, 140402(R) (2008).

[39] G. Meier, M. Bolte, R. Eiselt, B. Krüger, D.-H. Kim, and P. Fischer, Phys. Rev. Lett. **98**, 187202 (2007).

[40] C. Burrowes, A. P. Mihai, D. Ravelosona, J.-V. Kim, C. Chappert, L. Vila, A. Marty, Y. Samson, F. Garcia-Sanchez, L. D. Buda-Prejbeanu, I. Tudosa, E. E. Fullerton, and J.-P. Attané, Nat. Phys. **6**, 17 (2010).

[41] R. Moriya, L. Thomas, M. Hayashi, Y. B. Bazaliy, C. Rettner, and S. S. P. Parkin, Nat. Phys. **4**, 368 (2008).

[42] M. Hayashi, L. Thomas, C. Rettner, R. Moriya, and S. S. P. Parkin, Appl. Phys. Lett. **92**, 162503 (2008).

[43] M. C. Hickey, D.-T. Ngo, S. Lepadatu, D. Atkinson, D. McGrouther, S. McVitie, and C. H. Marrows, Appl. Phys. Lett. **97**, 202505 (2010).

[44] S. Lepadatu, J. S. Claydon, C. J. Kinane, T. R. Charlton, S. Langridge, A. Potenza, S. S. Dhesi, P. S. Keatley, R. J. Hicken, B. J. Hickey, and C. H. Marrows, Phys. Rev. B **81**, 020413 (2010).

[45] L. Thomas, M. Hayashi, X. Jiang, R. Moriya, C. Rettner, and S. S. P. Parkin, Nature **443**, 197 (2006).

[46] J. Xiao, A. Zangwill, and M. D. Stiles, Phys. Rev. B **73**, 054428 (2006).

[47] G. Tatara, H. Kohno, and J. Shibata, Phys. Rep. **468**, 213 (2008).

[48] Y. Tserkovnyak, H. J. Skadsem, A. Brataas, and G. E. W. Bauer, Phys. Rev. B **74**, 144405 (2006).

[49] K.-J. Lee, M. D. Stiles, H.-W. Lee, J.-H. Moon, K.-W. Kim, and S.-W. Lee, Phys. Rep. **531**, 89 (2013).

[50] M. Eltschka, M. Wötzel, J. Rhensius, S. Krzyk, U. Nowak, M. Kläui, T. Kasama, R. E. Dunin-Borkowski, L. J. Heyderman, H. J. van Driel, and R. A. Duine, Phys. Rev. Lett. **105**, 056601 (2010).

[51] D. Claudio-Gonzalez, A. Thiaville, and J. Miltat, Phys. Rev. Lett. **108**, 227208 (2012).

[52] http://micromagnum.informatik.uni-hamburg.de/.

[53] B. Krüger, A. Drews, M. Bolte, U. Merkt, D. Pfannkuche, and G. Meier, Phys. Rev. B **76**, 224426 (2007).

[54] An Oersted field along the observed direction most probably originates from the current flowing preferentially in the contact leads above the permalloy film [34], which is due to the higher electrical conductance of gold. The observed increase of the Oersted field on thickness reduction can be understood by considering the higher sputtering yield of gold compared with permalloy. As the thickness of the gold leads is reduced faster, the current distribution is shifted closer to the magnetic film and thus a larger Oersted field is sensed.